Adiabatically correcting an eddy–permitting model of the North Atlantic using large–scale hydrographic data

Carsten Eden[1,3], Richard J. Greatbatch[1] and Claus W. Böning[2]

[1] *Dalhousie University, Halifax, Canada*

[2] *Institut für Meereskunde, Kiel, Germany*

[3] *now at Institut für Meereskunde, Kiel, Germany*

Manuscript submitted to Journal of Physical Oceanography

Corresponding author address:
Carsten Eden
Institut für Meereskunde,
FB I, Theorie und Modellierung
Düsternbrooker Weg 20
24105 Kiel, Germany
email: ceden@ifm.uni-kiel.de

All figures are available in electronic format.

Abstract

The recently proposed "semi–prognostic method" adiabatically corrects flow properties of a hydrostatic ocean general circulation model (OGCM). We discuss four simple modifications to the semi–prognostic method and demonstrate their benefits in an eddy–permitting North Atlantic OGCM. The modifications successfully account for three drawbacks of the original method: reduced geostrophic wave speeds, damped meso–scale eddy activity and spurious interaction with topography.

Application of the modified method in the North Atlantic OGCM yields more realistic flow patterns and watermass characteristics in the Gulf Stream and North Atlantic current (NAC) and enhanced eddy kinetic energy. Biases of the uncorrected OGCM – too low northward heat transport and large–scale spurious surface heat fluxes due to false pathways of Gulf Stream and NAC – can be reduced by the modified method. The use of the corrected (eddy–permitting) OGCM, instead of the uncorrected, in a coupled climate model (as it now becomes possible, due to increasing computer power) might therefore allow a more realistic coupled simulation in certain regions of strong air–sea interaction. Since the method does not affect the tracer budgets directly, it is also well suited for a more realistic simulation of uptake and transport of passive tracers, such as anthropogenic CO_2 or components of ecosystem models.

1 Introduction

Any "useful" model of the ocean has to exclude processes, by either simply neglecting or parameterizing them, and contains therefore systematic errors. In a "good" ocean model, however, effects of these errors should be "small". In this study, the process under focus is the large–scale, time–mean circulation of the North Atlantic and the model under consideration is a standard, numerical, eddy–permitting ocean general circulation model (OGCM). We have in mind, as a possible application of the OGCM, a climate prediction framework, in which the ocean model is coupled to other components of the climate system, e. g. atmosphere and kryosphere. For decadal–scale integrations, present computational resources would allow to use horizontal resolutions in the ocean model nearly resolving the scales ($\sim$ 30 km) of the vigorous meso–scale motions in the ocean (eddy–permitting models). However, we are concerned that the ocean model under consideration might contain systematic errors due to effects of unresolved processes on the large–scale circulation which are not "small".

In a coupled climate model, a deficiency in one of the model components manifests itself in a drift towards an unreasonable climate (compared to the observed climate). The drifting climate of the coupled system becomes more and more different from the climate in each of the model components when driven in a stand–alone manner. The reason for the drift is, that the fluxes of momentum and buoyancy exchanged across the interface between the model components are biased by the systematic model errors. To prevent the coupled model from drifting, flux corrections are often used (Manabe and Stouffer, 1988), with the effect that only flux anomalies are exchanged while the mean states of the models are uncoupled. Obviously, such an approach is unsatisfactory and can produce defective results (Chen and Ghil, 1995).

In this study, we explore a method to correct the OGCM such that systematic errors are reduced (note, however, that, having the focus on the OGCM, we do not imply that other model components of the coupled system might not contain errors). The method which we use is based on the "semi–prognostic" method proposed by Sheng et al. (2001); a simple method to adiabatically change the advection properties of a hydrostatic OGCM by altering the pressure gradient in the momentum balance. The method can be viewed as a simple technique to assimilate hydrographic data into an ocean model, with the advantage over other simple methods, e. g. the robust diagnostic method of Sarmiento and Bryan (1982), that no spurious diabatic sources and sinks are introduced.

Sheng et al. (2001) applied the method with good success to a regional model of the northwestern Atlantic. Here, we extend the approach to a basin–scale application. Although the method performs well in improving the simulation of circulation patterns and watermass characteristics in the North Atlantic compared to observations, some problems arise in the model. Among them are changed dynamical properties of the semi–prognostic OGCM, for instance reduced Rossby wave speeds and damped eddy activity. We propose four modifications of the basic scheme to overcome these difficulties and demonstrate the benefits of the modifications in the model.

As an end product, we obtain an ocean model containing a fixed, non–flow–interactive correction term in the momentum balance, acting similar to a parameterization of effects of unresolved processes. The corrected model performs better in simulating realistic flow structures and watermass characteristics than the uncorrected OGCM, with the result that the corrected OGCM is better suited to be used in a coupled model system. Since the (adiabatic) correction does not affect the tracer budgets directly, it is also well suited for a more realistic simulation of the uptake and transport of passive tracers, as e. g. anthropogenic CO_2 or components of a pelagic ecosystem model.

This paper is structured as follows. In the second section we present the OGCM and review the semi–prognostic method, followed by a discussion of four modifications to the method. In the third section, we describe results from the prognostic OGCM in comparison to other eddy–permitting and

eddy–resolving models and discuss the application of the original semi–prognostic and the modified versions. The last section discusses our conclusions.

2 Ocean models and methods

2.1 Prognostic models

We apply the semi–prognostic method to an OGCM of the North Atlantic, part of the FLAME[1] hierarchy of models (Dengg et al., 1999), which includes versions of different resolution and different parameterizations of subgrid–scale processes. In all cases, however, the numerical code is based on a parallelized version of MOM2 (Pacanowski, 1995). The present study is based on a FLAME configuration, which we call the "eddy–permitting (FLAME) model", spanning the Atlantic Ocean from 20^oS to 70^oN with a horizontal resolution of $1/3^o \cos\phi$ (ϕ denoting latitude). The configuration is almost identical to the z–level model which was part of the European "DYNAMO" ocean model inter–comparison project (Willebrand et al., 2001). In particular, it uses the same horizontal resolution (eddy–permitting), the same surface boundary forcing (Haney–type heat flux condition as given by Barnier et al. (1995) and a restoring condition for sea surface salinity) and the same lateral boundary conditions (open boundaries after Stevens (1990) along 20^oS and a buoyancy restoring zone north of the Greenland–Iceland–Scotland ridge system and in the Gulf of Cadiz) as in DYNAMO. The main differences in the present FLAME setup are increased vertical resolution (45 levels) and therefore newly interpolated topography. In this study, we also change some of the physical parameterizations and numerical schemes. A third order tracer advection scheme (Quicker) replaces the traditional second order scheme (see Griffies et al. (2000) for the benefits) and a closure for the vertical turbulent kinetic energy following Gaspar et al. (1990) (utilizing identical parameters for the scheme as in Oschlies and Garcon (1999), see also a description of the model improvement therein) replaces a scheme proposed by Gargett (1984). Effects of unresolved processes in the momentum balance are parameterized, as in the z–level DYNAMO model, using biharmonic friction with viscosity of $2.5 \times 10^{11} \cos\phi \ m^4/s$. Explicit lateral diffusion is, in contrast to DYNAMO, set to zero; bottom friction is the same as in DYNAMO.

In each experiment the eddy–permitting FLAME model is integrated for a 10–year spinup period before being analyzed, if not otherwise noted. Annual mean model fields are obtained by averaging over a subsequent 3–year integration. The spinup period may appear short, if one considers that the bulk of the baroclinic adjustment of a North Atlantic model is believed to take place in 10–20 years. However, to explore the semi–prognostic method, we have decided to invest our restricted resources in several,

[1] See also *http://www.ifm.uni-kiel.de/fb/fb1/tm/research/FLAME/index.html*

shorter experiments with the eddy–permitting OGCM, instead of only a few, but longer experiments. For clarification, Fig. 1 shows the basin averaged kinetic energy in a 13–year long integration of the prognostic eddy–permitting FLAME model, giving an indication of the dynamical adjustment time scale in the model. Note that the time series in Fig. 1 saturates after about 10 year integration and shows no large trend for the 3 year analysis period.

For comparison we use results of the z–level DYNAMO model and an eddy–resolving FLAME model version. The latter model uses the same domain, same surface forcing and lateral boundary conditions and the same vertical resolution as the eddy–permitting FLAME model, but adopts a drastically increased horizontal resolution ($1/12^o \cos\phi$). Setup and spinup procedure of the eddy–resolving model is discussed in detail in Eden and Böning (2002), here we want to note the following caveat. The eddy–resolving FLAME model was initialized with the state of the eddy–permitting version at the end of a 15–year integration. The eddy–resolving version was then integrated for 8 years, subdivided in two periods, 3 years with high and 5 years with low viscosity and diffusivity. Results are shown here as 3–year averages from the end of the latter period. This integration may appear too short for a basin–scale baroclinic adjustment, but we think, nevertheless, that comparison aids the discussion in this study to show some effects of increased horizontal resolution, since it utilizes an identical configuration as the eddy–permitting model.

2.2 Original semi–prognostic method

Before describing the semi–prognostic method in detail, we want to motivate its name here in passing. A "prognostic" ocean model predicts momentum as well as the dynamical active density. In contrast, a "diagnostic" model is an OGCM in which potential temperature and salinity (density) are held fixed at certain climatological values. The momentum remains then as the only prognostic variable. There are certain disadvantages involved with such an approach, as discussed by, e. g. Greatbatch et al. (1991); Ezer and Mellor (1994). Due to small discrepancies between the prescribed baroclinic structure and the discretized model topography, large, spurious currents can occur since the density structure cannot be adjusted as in a freely evolving prognostic model. In an attempt to overcome this problem, model density is sometimes relaxed towards a climatology on a short time scale of order of days ("nudging"), which is then called a "robust diagnostic" model (Sarmiento and Bryan, 1982). However, it is obvious that unphysical sources and sinks of heat and salt are introduced by such an approach (Marotzke and Willebrand, 1996).

In a "semi–prognostic" model[2] (Sheng et al., 2001) the dynamical active density is given as a linear

[2]For being in between a diagnostic and prognostic model. One could also name it "semi–diagnostic". We prefer the optimistic way.

combination of an *a priori* known (in situ) density (ρ_c) and the density given by temperature, salinity (and pressure) calculated by the model using the equation of state (ρ_m):

$$\rho^* = \alpha\rho_m + (1-\alpha)\rho_c \tag{1}$$

It is the linear combination ρ^* which is used in the hydrostatic equation of a semi–prognostic model to calculate the pressure force in the baroclinic momentum equation. This is the only difference to a conventional, prognostic OGCM and is obviously readily implemented in numerical code. The parameter α ranges between zero and one. For $\alpha = 1$ we recover the prognostic model, for $\alpha = 0$ we get a diagnostic model and for values of the parameter between zero and one we get a semi–prognostic model.

Sheng et al. (2001) use monthly mean climatological values of temperature and salinity to calculate the *a priori* known density ρ_c. They estimate $\alpha = 0.5$ as an optimal value by comparison of modeled and observed currents. In the present study, we follow this route and take $\alpha = 0.5$ throughout the experiments. We also use monthly mean climatological temperature and salinity. However, in contrast to Sheng et al. (2001), who use a climatology of the northwest Atlantic (Geshelin et al., 1999), we use a combination of the global climatologies given by Boyer and Levitus (1997) and Levitus and Boyer (1994), serving also as the initial condition for the model. The seasonal cycle contained in the monthly mean $1^o \times 1^o$ climatology of Levitus and Boyer (1994) was extracted and carefully applied to the annual mean $1/4^o \times 1/4^o$ climatology of Boyer and Levitus (1997), in order to obtain both high temporal and spatial resolution. More details of the procedure are given in FLAME Group (1998)[3]. Results from the semi–prognostic model of Sheng et al. (2001) (which is similar to our OGCM in the present study, but restricted to the northwest Atlantic) are in several ways more realistic than results from the prognostic version of their OGCM. In particular, the circulation and watermass characteristics of the North Atlantic Current (NAC) east of the Grand Banks fits better to observations in the semi–prognostic version. The less realistic simulation of this region in the prognostic version of the model is common to similar models of the North Atlantic and a well known deficiency of z–level models (Willebrand et al., 2001). We show in section 3 that the same deficiency occurs in our prognostic OGCM and is improved in the semi–prognostic version of the model.

We want to stress that the success of the method, especially in improving the watermass characteristics is by no means trivial, since the tracer equations are unchanged in the semi–prognostic model, i. e. no artificial sources or sinks of tracers are introduced ("nudging") (Sarmiento and Bryan, 1982). Note that the method is also different from "momentum nudging", as used by e. g. Woodgate and Killworth (1997) and Stutzer and Krauss (1998). In the semi–prognostic method there are no

[3]This report can be accessed at *ftp://ftp.ifm.uni-kiel.de/pub/FLAME/WebDownload/Reports/FLAME_Rep98.ps.gz*.

artificial Newtonian relaxation terms added to the primitive equations. On the other hand, and for the same reason, the success of the method, or the convergence to a more realistic model state, is not guaranteed. Differences between model density ρ_m and climatological density ρ_c are driving changes in the advective flow due to changes in the momentum balance. But, this changed flow may not lead to a smaller difference between ρ_m and ρ_c, i. e. a more realistic ρ_m. However, we have never encountered a diverging solution in a semi–prognostic model; in all of our applications the method converges to a more realistic mean model state and appears surprisingly robust. This holds also for the modified versions of the method, which we discuss next.

2.3 Modifications to the semi–prognostic method

There are certain drawbacks of a semi–prognostic model, which we want to address and resolve in this study with modified versions of the method.

i) The pressure forcing in the momentum balance in the semi–prognostic model can be written as

$$\nabla p = g\nabla \int_z^0 dz \;\; (\alpha\rho_m + (1-\alpha)\rho_c) = \alpha\nabla p_m + (1-\alpha)\nabla p_c$$

introducing the pressure variables $p_m = g\int_z^0 dz \;\; \rho_m$ and $p_c = g\int_z^0 dz \;\; \rho_c$ and neglecting the contribution from the surface pressure. Considering now linear waves (small pertubations of a mean state in balance with the "forcing" term $(1-\alpha)\nabla p_c$) it becomes clear that waves must be affected by α, i. e. it is easy to show that baroclinic gravity wave speeds are reduced by a factor $\sqrt{\alpha}$. This means that, for instance, long (flat bottom) Rossby wave speeds are reduced by α and baroclinic Kelvin wave speeds by $\sqrt{\alpha}$.

ii) For the same reason, anomalous geostrophic velocities, i. e. geostrophic eddies, are reduced by a factor α. It is reasonable to expect, therefore, a similar damping influence on eddy kinetic energy.

iii) Especially in regions of strong boundary currents, interaction of the semi–prognostic method with the model topography can produce spurious up– and downwelling, affecting large–scale flow properties. We will show and further explain this effect in section 3.

We want to note, that i) and ii) can be utilized as an analysis tool. Eden and Greatbatch (2002) use the diagnosed, monthly mean *model* density after a spinup phase of a prognostic North Atlantic model as the prescribed density ρ_c (instead of an observed, climatological density) in a semi–prognostic version of the model. The effect is that the mean state of the semi–prognostic model is unchanged (with

respect to the prognostic version). But, since i) and ii) still hold, Eden and Greatbatch (2002) are able to quantify the role of geostrophic waves and anomalous advection, in their case for the ocean's response to changing surface forcing.

However, for the purpose of a realistic simulation of the ocean such effects appear undesirable. A straightforward way to overcome the problems i) and ii) is to diagnose the correction in Eq. (1) and to apply a corresponding non–flow–interactive correction in a subsequent integration. Eq. (1) can be written as

$$\rho^* = \rho_m + (1 - \alpha)(\rho_c - \rho_m) \tag{2}$$

We simply diagnose (by calculating over three years a monthly climatology of $(1-\alpha)(\rho_c-\rho_m)$) the second term on the rhs of Eq. (2) in a semi–prognostic model experiment. In the subsequent integration, we add these averages to the model density ρ_m in the hydrostatic equation of the model, which then corresponds to a non–flow–interactive forcing term in the momentum balance. This (monthly varying) forcing term will contain the corrections made to the model by the semi–prognostic method, with the difference that the correction is not flow–interactive anymore. We may argue that this correction accounts for errors of the prognostic model and call this kind of model a **"corrected–prognostic"** model. We demonstrate such an approach with our eddy–permitting OGCM in section 3. Note that a corrected–prognostic model is "fully prognostic" again and the influence of the semi–prognostic method on waves, anomalous advection and eddy kinetic energy is absent. The only difference to the conventional, prognostic model is that we have derived a correction term in the momentum balance which accounts for the systematic errors of the model. In effect, this correction behaves similar to a parameterization accounting for unresolved processes which would lead, without correction or parameterization, to systematic errors in the model.

However, to derive this correction term, it would be of benefit to have a semi–prognostic method, which relies only on the large–scale density structure, while the baroclinic meso–scale structures remain unaffected. This would reduce or eliminate the damping influence on the resolved eddy activity in the model. It is also likely that errors (e. g. measurement errors, geophysical noise by meso–scale eddies or insufficient smoothing techniques in the data processing) in the climatology used for the prescribed density ρ_c show up predominantly on smaller scales. For this reason it would be as well desirable to use only the large–scale features of the climatology density in the semi–prognostic method.

We propose two different approaches to realize such a semi–prognostic method. The first relies on spatial averaging, the second on temporal averaging. To formulate the first, we add to Eq. (1) a scale selective operator P, acting on the difference between dynamical active density ρ^* and model

calculated density ρ_m:

$$\rho^* = \rho_m + (1-\alpha)(\rho_c - \rho_m) + P(\rho^* - \rho_m) \tag{3}$$

P is supposed to be very large on small scales and very small on large scales. For the large scales we recover the original semi–prognostic method, i. e. Eq. (1), and for the small scales we get $\rho^* - \rho_m = 0$, thus no effect of the method[4]. $P = L^2\nabla^2$ (or $P = L^4\nabla^4$) satisfies this condition, where ∇ denotes the two–dimensional, horizontal nabla operator, and L a length scale, separating between the damping and the negligible influence of P.

To illustrate the benefit of Eq. (3) we show a simple one–dimensional example in Fig. 2. The upper solid line in the figure denotes the model density ρ_m, the lower solid line the climatological density ρ_c. There are small scales features in both densities, which are meant to resemble either a meso–scale eddy (for ρ_m) or a data error (for ρ_c). The dashed line in the middle shows the active density ρ^* using Eq. (1) with $\alpha = 0.5$. Both bumps, which we have built in the densities, show up in ρ^*, which contains then the "eddy" and the "data error". However, note that the amplitude of the "eddy" in ρ_m is reduced by half. Using Eq. (3) to calculate ρ^* (with $P = L^2\nabla^2$, the thick solid line in the figure denotes the length scale L) yields the dotted line, in which the "data error" in ρ_c is damped away and the "eddy" from ρ_m is more or less preserved, while the large–scale gradient of ρ^* remains still the same.

For the practical implementation of Eq. (3), it is necessary to solve as many Helmholtz equations as there are vertical levels in the OGCM for each time step. Since this is a heavy load for the computing costs, we use a moving average over several grid points in each horizontal direction (with equal weights as the simplest choice) as an approximation to the operator P. Using a moving average in the simple example in Fig. 2, yields very similar results as for $P = L^2\nabla^2$ (not shown). Tests reveal, that this approximate form of P produces also essentially the same results as the full operator in the OGCM, while only marginally increasing the computing costs. In the following, we call this method the **"smoothed" semi–prognostic** method.

The second version of a semi–prognostic method which prevents damping of eddy activity, is realized by temporal averaging. We simply average the second term on the rhs of Eq. (2) for a certain period. Assuming that eddies in the ocean have preferred time scales less than the averaging period, we filter out their influence in the correction. On the other hand, short–term variability, i. e. eddies, can then freely evolve in the OGCM, subject to the averaged correction term. We use simple one–year

[4]Note, that it is also possible to construct a method which acts predominantly on small scales while being negligible on large scales. Such an approach would be a simple method for, e. g. assimilating meso–scale signals into an (eddy–permitting) ocean model. However, we do not explore this route in the present study.

averages in the experiment discussed here, to bypass effects of the seasonal cycle. In other words, the term $(1-\alpha)(\rho_c - \rho_m)$ is averaged over the first year of the integration and added to the model density ρ_m in the second year, while further averaging the corresponding value during the second year, which is applied in the third year, and so forth[5]. We call this version the **"mean" semi–prognostic** method. We do not filter out possible small–scale data errors with the mean semi–prognostic method as before with the smoothed semi–prognostic method. However, a combination of smoothed and mean method can certainly be used.

Finally, the remaining caveat is iii), a possible interaction of the semi–prognostic method with topography, causing spurious up– and downwelling. One reason for this effect is that the climatological density may not imply a (geostrophically balanced) continuous boundary current. This can be a result of the interpolation and smoothing techniques used for the compilation of the climatology; e. g. the slopes of the isopycnals across the boundary current might be reduced. This appears to be the case for example in the Gulf Stream of the climatology of Boyer and Levitus (1997), as our experiments suggest. To overcome this problem, we have tapered the parameter α near the boundaries to one, which means that the model becomes "locally prognostic" in calculating the boundary current system and semi–prognostic in the interior. We call this method the **"tapered" semi–prognostic** method. Note that it appears also possible, to exclude e. g. the deep ocean from having influence on the method by setting α to one below a certain depth, since there, observations might be less reliable.

In summary, to resolve the difficulties i) to iii) we propose four modifications to the original semi–prognostic method. Spatial averaging (smoothed method) or temporal averaging (mean method) of the correction term in the semi–prognostic model is applied to reduce the damping influence on eddy activity. Possible data problems near the boundaries (or deep ocean) are accounted for by relaxing there the influence of the method (tapered method). Having done a spinup integration with one or a combination of these modified methods in a semi–prognostic model, we proceed by diagnosing the correction term and applying it as a non–flow–interactive correction in the subsequent integration (corrected–prognostic), which finally resolves the problem of modified physical properties.

3 Results

We have performed various experiments with the above described semi–prognostic methods applied to the eddy–permitting OGCM. In order to present the essential results of the experiments, we focus on

[5]Note that a "smoother" method can be obtained using a moving average over, e. g. the model time steps, of one year. Using this moving average instead of the discrete annual averages, would eliminate the otherwise sudden change in the correction at the end of each year, but is, however, computationally very elaborate. Therefore, we stick to the former averaging method. Note also that a possible variation is the use of ensemble averages of the OGCM instead of temporal averages, but, we do not explore this route in the present study.

a few key points in the circulation of the northern North Atlantic and discuss and compare selected prognostic and semi–prognostic model results. These key points are the upper level flow of the North Atlantic Current (NAC) around the Grand Banks south–east of Newfoundland and the flow of the Gulf Stream, from its separation from the shelf to the Grand Banks. We also compare important large–scale features of the model, i. e. northward heat transport, meridional overturning circulation, and distribution of upper level EKE, to describe the model performance. However, to start, we discuss the surface air–sea flux as diagnosed in the prognostic models to point out possible systematic model errors.

3.1 Prognostic models

Figure 3a) shows the annual mean heat flux as given by a 3–year analysis period of the ECMWF numerical weather forecast model (Barnier et al., 1995). According to this figure, the northern North Atlantic is loosing heat almost everywhere with maximum heat loss along the path of the Gulf Stream and the NAC southeast of Newfoundland, the central Labrador Sea and Irminger Sea. Areas of (small) heat gain are located in the upwelling regions off the coast of North Africa and over the shallow Grand Banks east of Newfoundland. As for the DYNAMO models, the surface heat flux boundary condition for our OGCM is given as the (however monthly varying) flux of Fig. 3a) plus, following Barnier et al. (1995), a relaxation term, derived from linearized bulk formulas and accounting for a possible deviation of the modeled Sea Surface Temperature (SST) from a observed, climatological one. Therefore, the flux in Fig. 3a) may not coincide with the heat flux which enters our OGCM. In the case of a systematic model error which shows up in the modeled SST, we expect a significant, large–scale contribution in a longer–term average of the relaxation term. On the other hand, interpretation of the relaxation term must be careful, since the surface forcing, either wind stress or buoyancy fluxes (or other components of the model setup), might also contain errors and show up (directly or indirectly by apparently false ocean model results) as well in the relaxation term.

Fig. 3b) shows the diagnosed heat flux from the prognostic eddy–permitting model after the spinup, containing both the relaxation term and the net surface heat flux from ECMWF. It is clear from Fig. 3b) that there is a significant large–scale contribution of the relaxation term along the path of the NAC around the Grand Banks, causing the most prominent difference to the ECMWF heat flux. We show in Fig. 3c) the diagnosed heat flux from the z–level DYNAMO model as well. The DYNAMO model shows a similar contribution at the same location, pointing towards a common feature in the models.

Fig. 4a) shows the long–term mean observed temperature (Boyer and Levitus, 1997) at 50 m depth around the Grand Banks. Evidently, there is a strong signature of the NAC flowing northwards parallel

to the Grand Banks, with warm water of subtropical origin to the right and cold subpolar water to the left, until it penetrates eastward into the interior North Atlantic at about 52^oN. Fig. 4b) shows mean temperature and velocities at the same depth in the prognostic model. Clearly, there is almost no northward flow east of the Grand Banks in the prognostic model, which leads to too cold water compared to the observations, north of about 46^oN and, in consequence, to the large contribution to the relaxation term of the surface heat flux. Therefore, we conclude that the contribution of the relaxation term in this region shows a significant systematic error of the OGCM. Second, we can assume that this is not just an artifact of our specific model, but a common problem in this class of eddy–permitting models of the North Atlantic, as previously noted by Böning et al. (1996) and by Willebrand et al. (2001) for the DYNAMO (level) model showing a similar deficiency.

Coupling such an ocean model to an atmospheric general circulation model, would likely raise the need for a flux correction at this location. However, this region (sometimes referred to as the "storm formation region") is of potential importance for a coupled model, since here, strong lower level baroclinicity is created in the atmosphere by the warm SST, supporting growing disturbances and influencing the storm track in the North Atlantic. Therefore, we think that the spurious flow around the Grand Banks in the OGCM points towards a potentially important problem in realistic, high resolution coupled models. We attempt to reduce this model artifact with our semi–prognostic methods and propose to use a corrected–prognostic model in a coupled model system.

3.2 Original semi–prognostic model

In the semi–prognostic models the flow around the Grand Banks is more realistic. Fig. 4c) shows mean temperature and velocities at 50 m depth in an experiment applying the original semi–prognostic method in the eddy–permitting OGCM. Water north of 46^oN is up to 8^o warmer than in the prognostic version. In fact, the circulation is now getting similar to model solutions with drastically increased horizontal resolution. Fig. 4d) shows mean temperature and velocities for the eddy–resolving model in this region, agreeing surprisingly well with the semi–prognostic model. The northward migration of the northern boundary of subtropical water east of the Grand Banks coming along with increased horizontal resolution, as observed here for the FLAME models, is also reported by Smith et al. (2000) (their Fig. 9b and c). Thus, for a more realistic simulation of this region, i. e. the correct flow pattern of the NAC, it appears necessary to use very high horizontal resolution in the OGCM, presently too costly for use in a coupled modelling system. However, the semi–prognostic model produces a similar degree of realism using much less resources. Carrying over this improvement to a corrected–prognostic version of the model would be therefore of great benefit.

Further upstream of the NAC, we meet another region in which eddy–permitting North Atlantic

models usually fail to simulate realistic flow patterns and watermass structure. This is the Gulf Stream from its point of separation from the shelf near Cape Hatteras to the Grand Banks. Fig. 5 shows in this region the observed temperature (a) and modeled temperature and velocity in the prognostic model (b), the semi–prognostic model (c) and the $1/12^o$ model (d). We see for the prognostic eddy–permitting model as well as for the eddy–resolving model too warm water at the northern flank of the Gulf Stream. Furthermore, there are strong recirculation cells near the separation from the shelf. The latitude of separation appears too far to the north. In the interior, the stream does not show a jet–like structure, but, in contrast, several flow paths, most of them too far to the north, leading apparently to the too warm water north of the Gulf Stream. This is in agreement with results from many previous model solutions and in contrast to observations, as described by Dengg et al. (1996). Note, however, that while the FLAME eddy–resolving model fails to simulate a realistic Gulf Stream, other high resolution OGCM's are able to produce realistic simulations (Smith et al., 2000; Paiva et al., 1999).

In the semi–prognostic model, the situation is again more realistic than in the prognostic version; there is a distinct jet–like flow to the Grand Banks. Although we see still an unrealistic recirculation cell near Cape Hatteras, it is much smaller in amplitude compared to the prognostic model. Furthermore, temperatures north of the flank of the Gulf Stream are now several K cooler than in the prognostic model and in much better agreement with the observations.

The improvements, shown by the semi–prognostic model with respect to the prognostic model, in simulating more realistically some of the major flow patterns in the North Atlantic give some hope that the spurious anomalies in the surface heat fluxes due to systematic model errors are now reduced. It turns out, however, that the improvements are not as large as expected. Fig. 3d) shows the diagnosed heat flux for the semi–prognostic model. Comparison with Fig. 3b) shows that we now find heat loss east of the Grand Banks with maximum amplitude of 60 Wm^{-2}, but still less than in the ECMWF heat flux where the heat loss reaches 100 Wm^{-2} and covers a broader region. Moreover, we see also a region of heat gain north of 50^oN.

This result points towards too little northward transport of warm water in the semi–prognostic model. Fig. 6 shows the mean northward heat transport for the prognostic, the semi–prognostic, the DYNAMO model and the eddy–resolving model. While heat transports in the prognostic, eddy–permitting FLAME and DYNAMO models are similar[6], the eddy–resolving model shows in general more and the semi–prognostic model less northward heat transport. Also shown are observational estimates derived from hydrographic data by MacDonald and Wunsch (1996) and Ganachaud and

[6]The (maybe spurious) heat uptake between about 30^oN and 40^o in DYNAMO in contrast to the (more reasonable) heat loss in FLAME is most likely due to different mixed layer schemes. There was none in DYNAMO, while FLAME uses a TKE scheme. See also the difference in heat fluxes in the eastern, subtropical North Atlantic in Fig. 3b) and c).

Wunsch (2000) and derived from atmospheric data by Trenberth and Caron (2001). Since the observations show a large spread within approx. 10^o of the equator and our main focus is on the mid–latitude North Atlantic, we omit here a discussion of possible model (forcing, data) errors in the tropical Atlantic. However, it is evident that the eddy–permitting models show a bias in carrying too little heat northward compared to the observations, while the eddy–resolving model shows stronger northward heat transport. Note, that the enhanced heat transport in the eddy–resolving model coming along with increased resolution, is in agreement with the model results discussed by Smith et al. (2000). However, more realistic flow patterns and watermass characteristics in the semi–prognostic model do not lead to a similar effect as increased resolution; in contrast, the bias to unrealistic low northward heat transport is enhanced in the semi–prognostic model.

The major agent to transport heat northward in the North Atlantic is the meridional overturning circulation (Böning et al., 1995). Fig. 7 shows the meridional streamfunction for the prognostic (a) and the semi–prognostic model (b). In the prognostic model, we see around 45^oN maximum northward volume transport in the upper 1000 m of about 14 Sv. A similar amount is transported in the semi–prognostic model at this latitude, but strong upwelling between 30^oN to 35^oN, reduces the northward volume transport south of 30^oN to about 8–9 Sv in the semi–prognostic model. In the prognostic model, the upwelling is not as strong, 10–11 Sv are still carried northward south of 30^oN. The strengthened shortcut of the overturning circulation by the enhanced upwelling in mid–latitudes in the semi–prognostic model compared to the prognostic model, leads apparently to the bias towards low heat transport.

The semi–prognostic, and to a lesser extent the prognostic model, are suffering both from a long known model artifact, the so called "Veronis–effect". As first described by Veronis (1975), horizontal diffusion in OGCM's generates diapycnal buoyancy fluxes in the presence of steep slopes of isopycnals. Strongly inclined isopycnals can be found in western boundary currents, most prominent in the Gulf Stream. Here, the diffusive diapycnal buoyancy fluxes across the front of the current are balanced by vertical advective transports, showing up as the spurious (cold) upwelling in the meridional streamfunction and reducing the northward heat transport in consequence. This model artifact can be effectively reduced by the use of isopycnal diffusion, i. e. tracer diffusion oriented along isopycnals (Böning et al., 1995; Griffies, 1998). Apparently, the (small, flow–interactive) implicit, numerical diffusion of the advection scheme (Quicker) used for the eddy–permitting OGCM acts more like horizontal diffusion instead of isopycnal diffusion, leading in the prognostic model to the upwelling south of 35^oN of about 3 Sv. We want to note here in passing, that in a version of the same eddy–permitting model using the (traditional) 2. order centered differences advection scheme together with (explicit) isopycnal diffusion, the upwelling effect is reduced compared to the version with Quicker and without explicit

diffusion, coming along with a stronger overturning circulation and with increased northward heat transport. On the other hand, the "isopycnal" version shows almost entirely suppressed eddy activity and less realistic flow of the Gulf Stream and NAC (both not shown) compared to the version with the Quicker advection scheme. However, we make no further use of the "isopycnal" model version (neither prognostic nor semi–prognostic) in the present paper.

In the semi–prognostic model, as shown in Fig. 7b), the Veronis effect is enhanced. We may have indirectly changed the diffusive buoyancy transports with the method, by changing the advective flow and therefore the implicit, numerical diffusion. However, we regard this diffusive effect as minor, compared to vertical velocities which we might generate, using the semi–prognostic method near boundaries with steep isopycnals as in the Gulf Stream region. Here, the climatological density ρ_c which we use, contains apparently information about the boundary current transport (caveat iii) in section 2.3), inconsistent with the model. The resulting inconsistency is then accounted for by spurious up(– or down)welling near the western boundary (not shown), leading to the enhanced Veronis effect as seen in Fig. 7b). Note that using the smoothed and/or tapered semi–prognostic methods, the (inconsistent) information about the (small–scale) slopes of the boundary current is essentially excluded from having influence, with the effect of reduced spurious upwelling, as we shall show below in section 3.3, confirming this interpretation.

In contrast to the prognostic model, there are also strong recirculation cells in the meridional streamfunction of the semi–prognostic model around the equator below about 2500 m with a maximum at about 4000 m. The reason is another interaction between topography and semi–prognostic method. The topography of the model allows[7], through a small gap in the Mid Atlantic Ridge system at the equator (the model representation of the Vema and Romanche Fracture Zone), for an cross–equatorial flow east of 25^{o}W below 4000 m. In the climatology of Boyer and Levitus (1997) we find in the eastern, equatorial region in the Atlantic below 4000 m cool and fresh water south of the equator (resembling Antarctic Bottom Water) and relatively warm and saline water north of the equator (more akin to North Atlantic Deep Water). Apparently, the modeled (northward) transport through the Vema and Romanche Fracture Zone is unrealistic: both, prognostic and semi–prognostic model deviate from the observations, i. e. showing cooler and fresher water than in the observations on the northern side of the gap, and warmer and more saline on the southern side (not shown), pointing towards a too strong deep cross–equatorial flow into the eastern North Atlantic.

The semi–prognostic method generates corrective pressure gradients in the deep, eastern equatorial region due to large deviations from the climatology, which however, do not lead to an improvement

[7]In fact, the topography of the eddy–permitting FLAME model was manipulated by hand after discretization to allow for this throughflow (Kröger, 2001). Similar hand–tuning was applied at several other location, e. g. the Denmark and Florida Strait.

in the model density, since transports across the Vema and Romanche Fracture Zone are apparently unchanged. The corrective pressure gradients are largest at the narrow throughflow point at the equator, leading to the spurious recirculation cells between 2500 m and 4500 m in Fig. 7b). Clearly, this result points to another potential problem of a semi–prognostic model. A simple way to resolve that problem is to manipulate the topography in this region and to inhibit the artificially strong throughflow. However, we have not made such an attempt, since the modified versions of the method take care of this problem, as we shall show below.

In summary, we see that the semi–prognostic model performs well in improving the simulation of major advective pathways and, consequently, watermass structures of the North Atlantic, but we encounter problems (in addition to reduced wave speed and damped meso–scale activity). First, there is stronger upwelling in the Gulf Stream region compared to the prognostic model, leading to a reduction of northward heat transport. Second, there are potential problems near the topography. By spurious transports through artificial gaps, large corrective pressure gradients can build up, which are unable to improve the solution. We show in the next section that the modified semi–prognostic methods are able to resolve these problems.

3.3 Smoothed, mean and tapered semi–prognostic models

We discuss in this section results from experiments with the modified semi–prognostic methods. The main experiments in this section are the following:

- Experiment MEAN, in which the *mean* semi–prognostic method is applied in the same manner as explained in section 2.3.
- Experiment SMOOTH, applying both the *smoothed* and *tapered* semi–prognostic method. The moving average involves 10 grid points in each direction (equal weights) and within 6 grid points distance from land, the parameter α is set to 1 (and to 0.5 everywhere else).
- Experiment MEAN+SMOOTH, in which MEAN and SMOOTH are combined, i. e. the averaged correction of the mean method is smoothed and tapered as the instantaneous correction in SMOOTH.
- Experiment MEAN+SMOOTH-800, repeating MEAN+SMOOTH with the difference that here the moving average involves only 5 grid points and α is tapered within three grid points distance from land. Moreover, α is set to 1 below 800 m.

We remind the reader that spinup and analysis procedure and other details are discussed in section 2.1 and that in all cases the methods are applied to the eddy–permitting FLAME model.

To start, we confirm that the mean and smoothed methods reduce the damping influence of the original semi–prognostic method on eddy activity. Fig. 8a) shows Eddy Kinetic Energy (EKE) at 50 m depth in the prognostic eddy–permitting OGCM. Maxima of EKE show up in the Gulf Stream region and along the path of the NAC, smaller local maxima in the Labrador Sea and the Irminger Sea. It must be noted that there is a bias of too low EKE in eddy–permitting OGCM's in mid–latitudes (Smith et al., 2000; Eden and Böning, 2002); eddy–resolving OGCM's and observational estimates show order of magnitude higher levels. The reason is insufficient horizontal resolution to capture the bulk of the essential hydrodynamic instability processes in eddy–permitting models. On the other hand, the horizontal distribution of near surface EKE in eddy–permitting OGCM's in general agreement with observational estimates (Stammer et al., 1996).

As expected, EKE is damped in the model using the original semi–prognostic method, as Fig. 8b) reveals. The basin–wide average of EKE at 50 m depth is $63 \times 10^{-4}\ m^2 s^{-2}$ and $36 \times 10^{-4}\ m^2 s^{-2}$ for the prognostic model and the model utilizing the original semi–prognostic method, respectively. On average, upper level EKE is thus reduced by half with the original semi–prognostic method. However, the mean and smoothed versions of the method recover (and exceed) the level of EKE in the prognostic version. Fig. 8c) and d) show the corresponding results from MEAN and SMOOTH. In both figures, maxima of EKE are similar to the prognostic model, showing the success of both methods. The basin average of EKE at 50 m depth are $84 \times 10^{-4}\ m^2 s^{-2}$ for MEAN[8] and $68 \times 10^{-4}\ m^2 s^{-2}$ for SMOOTH. The reason for the excess of EKE in MEAN is that MEAN shows enhanced values of EKE compared to the prognostic model in the more quiescent regions, like the eastern subtropical North Atlantic. This is not the case for SMOOTH, but, only minor differences in the maxima of EKE show up compared to MEAN. Furthermore, mean and smooth method lead clearly to a northward migration of maximum EKE east of Newfoundland, pointing towards more realistic flow of the NAC in this region.

EKE in MEAN+SMOOTH (not shown) is similar to SMOOTH, the basin average of EKE at 50 m depth is $69 \times 10^{-4}\ m^2 s^{-2}$, while EKE in MEAN+SMOOTH-800 (where we have reduced the length scale, and therefore the influence, of the moving average) is more akin to MEAN, with a basin average of EKE of $73 \times 10^{-4}\ m^2 s^{-2}$. The differences suggest that the temporal averaging in MEAN is superior in preserving EKE in a semi–prognostic model, compared to the spatial averaging. However, both methods are successful in that respect, i. e. the level of EKE in the prognostic model is at least recovered in all experiments with the modified semi–prognostic methods.

[8]Note that we get similar (or even higher) ratios of EKE in MEAN compared to the other experiments, restricting the calculation of EKE to the second half of each year of the analysis period, thus excluding the barotropic and inertial adjustment to the changing correction term in MEAN.

Most of the improvements of the original semi–prognostic with respect to flow patterns in the Gulf Stream and NAC are carried over to the mean, smoothed and tapered methods. Fig. 9a) exemplifies the flow of the NAC around the Grand Banks in the experiments with the modified semi–prognostic method. The figure shows results from MEAN, the other experiments are akin. The temperature distribution and flow pattern is similar to the results of the original method (Fig. 4c) showing that we can achieve the same effect in this region with the modified versions as with the original version without affecting the small–scale variability. Note that we see even slightly warmer water north of about 48^oN (more similar to the eddy–resolving model) most likely due to enhanced mixing across the front by meso–scale variability in the modified versions.

Fig. 9b) shows the simulation in MEAN for the Gulf Stream region. In contrast to the original semi–prognostic model, we see now an almost vanishing spurious recirculation cell at the separation point and, as before, a jet–like flow to the southern tip of the Grand Banks. The temperature distribution is again in good agreement with Boyer and Levitus (1997). The success of the mean semi–prognostic method in eliminating the recirculation cells can be understood in the following way. If such a recirculation cell is developing in the course of a year, the averaged correction is accounting in the next year for that deviation of model density from the climatological density, i. e. by redirecting the flow, which will tend to reduce the potential energy, stored in the spurious cell. Thus, on average, the mean semi–prognostic method tends to damp out spurious, standing eddies. It must be noted, however, that in the other experiments with modified versions the simulation with respect to the separation is inferior to MEAN; i. e. in the tapered experiments we see stronger recirculation cells than in MEAN. Clearly, the reason is the missing (in SMOOTH) or reduced (in MEAN+SMOOTH) damping influence on standing eddies of the mean semi–prognostic method. However, there is still, as in MEAN, a jet–like flow of the Gulf Stream in the interior after separation (not shown) in the other experiments.

Flow patterns and watermass characteristics of MEAN+SMOOTH-800 are almost identical to MEAN+SMOOTH (not shown), revealing two results. First, sensitivity to the length scale of the smoothing operator P (moving average) is apparently small, except for EKE, as discussed above. Second, using density in the upper ocean (roughly above the thermocline) only for the semi–prognostic method, appears to be sufficient to obtain the same benefits. In contrast, an experiment (not shown) applying the mean semi–prognostic method only in the upper 200 m, shows almost no difference to the original, *prognostic* model, while an experiment (not shown) applying the mean method from $200 - 800$ m recover almost the results of MEAN. The likely reason is that the greatest shear of geostrophic velocities, i. e. the flow component which is directly influenced by the semi–prognostic method, can be seen in the thermocline.

Fig. 9c) shows the diagnosed surface heat flux from MEAN+SMOOTH-800. We see that the strong heat gain east of Newfoundland, as found in the prognostic eddy–permitting models, has now almost disappeared. Clearly, the situation with respect to this model artifact has also improved compared to the original semi–prognostic model. MEAN, SMOOTH and MEAN+SMOOTH are all very similar to Fig. 9c), confirming the benefit of the modified versions.

However, differences in the experiments with the modified methods show up in the meridional heat transport, shown in Fig. 10a). In SMOOTH, MEAN+SMOOTH and MEAN+SMOOTH-800, there is an increase in heat transport compared to the prognostic model, most pronounced, about 0.1 PW at maximum, in MEAN+SMOOTH and MEAN+SMOOTH-800. MEAN shows less heat transport; however, it is still more than using the original semi–prognostic method. The reduced heat transport in MEAN comes along with weaker overturning circulation south of 30^oN due to stronger upwelling near 35^oN (not shown) compared to the prognostic model; the same deficiency as we have seen for the original semi–prognostic method, here, however, slightly reduced.

In contrast, the other (smoothed and tapered) experiments do not show this deficiency anymore. In MEAN+SMOOTH-800 the maximum northward volume transport south of 30^oN is enhanced by 1 Sv compared to the prognostic model. The upwelling (Veronis effect) is reduced, although still present, as Fig. 10b) reveals. The corresponding streamfunction for MEAN+SMOOTH (not shown) is very similar to the one in MEAN+SMOOTH-800; in SMOOTH (also not shown) its shape is similar to Fig. 10b), but with reduced (about 1 Sv) maximal amplitude. The mean method still includes all small–scale information in the climatological density, in particular the boundary current structure, while in the smoothed and tapered methods, these structures are effectively excluded. We can conclude, that it is the spatial smoothing and tapering of the semi–prognostic correction, which resolves the spurious upwelling in the Gulf Stream region (Veronis effect) as seen for the original method (and to a lesser extent in MEAN).

In summary, with respect to EKE both modified semi–prognostic versions (mean and smoothed) perform better than the original method, with larger EKE for the mean method, even larger than in the prognostic version. Improvements in flow patterns and watermass characteristics as given by the original method are carried over to the modified model, or are even outperformed. The same benefits can be obtained, applying the method above the thermocline only. Problems discovered for the original semi–prognostic method, involving interaction with topography are resolved with the modified versions. The spurious upwelling near the Gulf Stream separation is reduced using the smoothed and tapered methods. However, application of the mean method, without combination with the other methods, appears not as successful in this respect.

3.4 Corrected–prognostic models

Having established now the modified semi–prognostic methods, we finally present results from corrected–prognostic models in this section. The semi–prognostic correction is diagnosed and averaged in the analysis period of the experiments described above in section 3.3. This diagnosed, no longer flow–interactive, correction is applied to the model in the subsequent integration. All corrected–prognostic model experiments presented here, start from the end of the analysis period of the corresponding semi–prognostic models and last for 7 years, to allow for another baroclinic adjustment. Results are shown as averages over the last three years of that integration. We add the suffix "-CORR" to the names in section 3.3 to name the experiments, e. g. the experiment utilizing the correction of MEAN is called MEAN-CORR.

First we note, that there are no large trends over the integration period of the experiments described in this section, i. e. the solution of the modified semi–prognostic models remains almost unchanged, switching to the corrected–prognostic version. For clarification, Fig. 11 shows again the heat transport in MEAN, MEAN+SMOOTH and MEAN-SMOOTH-800 together with the corresponding corrected–prognostic experiments. We see that the heat transport in the corrected–prognostic versions remain at about the same level as in the corresponding semi–prognostic version. The same holds for the other so far discussed quantities, as EKE, overturning, flow patterns, etc.

Fig. 12 shows some examples of the solution of MEAN+SMOOTH-800-CORR. Overall, we see that the benefits of the original semi–prognostic model, as well as the modified versions are carried over to the corrected–prognostic models. However, despite the small increase in northward heat transport in MEAN+SMOOTH-800-CORR, a little more heat gain shows up north of about 50^oN compared to the corresponding modified semi–prognostic version (compare Fig. 9c), most likely due to a small southward shift of the NAC. However, there is still a large improvement in the pattern of the surface heat flux with respect to the prognostic model (compare Fig. 3b) and, in addition, up to 0.1 PW more northward heat transport in the corrected–prognostic model, which is now well inside the error estimates of the mid–latitude observations (compare Fig. 6a). Note that with the corrected–prognostic model we finally resolve also the problem of changed dynamical properties in the model (caveat i). This effect is readily demonstrated in idealized numerical and analytical models, but we do not make any attempt to show the effect in our realistic OGCM.

4 Concluding discussion

We have applied the semi–prognostic method as proposed by Sheng et al. (2001) to an eddy–permitting model of the North Atlantic. Our aim is to reduce systematic model errors, such as unrealistic upper level flow and watermass characteristics of the NAC around Newfoundland and the Gulf Stream region between Cape Hatteras and the Grand Banks, resembling long standing deficiencies in North Atlantic models. These deficiencies have been only recently and only in part resolved with highly increased horizontal (eddy–resolving) resolution (Smith et al., 2000). As for the regional model of Sheng et al. (2001), the semi–prognostic model version performs better than the prognostic version with respect to observations at these key points of the North Atlantic circulation. In fact, the semi–prognostic version is getting similar to an eddy–resolving model version in many respects. The improvement is achieved by applying a flow–interactive correction of the pressure gradient in the momentum budget, simply taken from hydrographic observations. Tracer budgets are not directly affected by the method, i. e. no diabatic sources and sinks of heat or salt are introduced.

However, we have noted three inherent drawbacks of a semi–prognostic model. These are changed dynamical properties of the model, i. e. reduced geostrophic wave speeds and damped meso–scale eddy activity, and spurious interaction of the method with topography. We have discussed and successfully applied four simple modifications of the original semi–prognostic method to overcome these drawbacks. By spatial averaging and/or temporal averaging of the semi–prognostic flow correction it is possible to include only the large–scale hydrographic information and to reduce the damping influence of the original method on eddy activity. In fact, eddy kinetic energy is even enhanced in the modified semi–prognostic models (more than 30% for the mean method) compared to the prognostic model. In combination with a relaxation of the flow correction near the coast, it is possible to overcome the spurious interaction with the topography. Restricting the flow correction furthermore to the upper ocean (roughly in the permanent thermocline), thus excluding the (eventually) less reliable[9] deep observations, reveals essentially the same benefits as using the flow correction everywhere.

Having done a spinup integration with one or a combination of the modified methods in a semi–prognostic model, we proceed by diagnosing the correction term and applying it in the subsequent integration (corrected–prognostic model), resolving the problem of modified physical properties and acting similar to a parameterization of unresolved processes in the OGCM. The benefits of the original semi–prognostic model, i. e. a better representation of the advective flow east of Newfoundland and in the Gulf stream region, are carried over to (or are even outperformed by) the modified semi–prognostic models and, finally, to our end–product, the corrected–prognostic model. We also note, that similar

[9]We mean by "less reliable" a potentially larger error at depth due a smaller number of observations, insufficient to filter out effects of eddy variability.

benefits of the method can be obtained in non–eddy resolving OGCM's, as experiments reveal with a version of our OGCM with coarser resolution ($4/3^o \cos\phi$), which are, however, not discussed in the present study.

Motivation for correcting the OGCM are large–scale spurious surface heat fluxes (compare Fig. 3) of models of the North Atlantic, recognized as a long standing deficiency in many previous model studies (Böning et al., 1996; Willebrand et al., 2001)), coming along with a bias of too low northward heat transport. In particular, spurious heat fluxes are related to a missing northward turn of the NAC as it flows southeast of Newfoundland, showing up in eddy–permitting OGCM's (but also, to an sometimes even larger amount, in non–eddy–resolving models). We argue, that using such an eddy–permitting (uncorrected) OGCM in a coupled model system, as it now becomes possible, might not improve the realism of the simulation, compared to the use of a non–eddy–resolving OGCM, at least in this ("storm track formation") region, which is of potential importance for air–sea interaction. The correction strategy for the OGCM presented in this study might allow to simulate the correct position of the subpolar front in the western North Atlantic, with benefits for the realistic coupled simulation of the atmospheric strom track in this region.

To quantify the effect, we calculate the horizontal average of the region east of Newfoundland (42^oW–30^oW and 42^oN–50^oN), in which the NAC looses large amounts of heat to the atmosphere, 57 TW according to the heat fluxes of the ECMWF analysis (Barnier et al., 1995). In contrast, the prognostic model *gains* 19 TW in this region, due to the missing northwest turn of the NAC, similar to e. g. the DYNAMO z–level model of Willebrand et al. (2001) and many other previous model solutions. The modified semi–prognostic model (MEAN+SMOOTH-800) reduces this systematic error through adiabatically changing the advective flow in this region by about 43%, the corresponding corrected–prognostic model by 25%, both leading now to an average heat loss of the model in this region. Furthermore, the total northward heat transport increases in the corrected–prognostic at maximum by about 0.1 PW (and to a similar extent in the modified semi–prognostic model) compared to the uncorrected prognostic model.

We must note, however, that since we are using a fixed, non flow–interactive correction of the large–scale properties of the model, based on historic hydrographic observations, the corrected–prognostic model is not well suited for coupled simulations with large deviations from the present climate. However, it should be well suited for simulations of the present climate state, e. g. seasonal to decadal–scale climate forecasts or hindcasts. In a simulation of, for instance, the last glacial maximum or serious climate changes due to greenhouse gas forcing, in which large deviations of the mean, large–scale oceanic flow can be expected, one has to fall back to the prognostic OGCM. On the other hand, flux–correcting the OGCM in such a coupled simulation contains information about the present climate state in a

very similar way as our approach, thus suffering from the same problem.

However, beside a coupled climate model, another attractive possible application of the method is the following. Since the correction in a semi–prognostic, or corrected–prognostic model does not affect the tracer budgets directly, it would be also well suited for the simulation of the advective, turbulent transport of a passive tracer in a realistic ocean model of the present climate state. Possible application are for example the simulation of the uptake of anthropogenic CO_2, coupling of the OGCM to pelagic ecosystem models, or oceanic now–and forecasts for industrial purposes, e. g. a simulation of the dispersal of pollutants.

Finally, we want to note that the semi–prognostic method is well suited to be used for a pragmatic two–way nesting approach. Especially the transfer of information from a nested model with enhanced resolution to a model of larger domain with coarser resolution is usually difficult to realize. But also constraining the nested model to match the coarser resolution model at its boundaries can cause problems, i. e. the nested model can get "decoupled" from its boundary conditions. Clearly, the semi–prognostic method is a simple and robust way to adiabatically pass large–scale information from the larger domain into the nested model and small–scale information of the nested model to the larger domain. We will explore this route in a future study.

Acknowledgments

This work has been supported by funding provided to the Canadian CLIVAR Research Network by NSERC, CFCAS and CICS. We are also grateful for the use of computer facilities of the Canadian Meteorological Centre in Dorval, Quebec, Canada. We acknowledge the contributions of the FLAME group at IfM Kiel, especially the work of J. Dengg and R. Redler. The integration of the eddy–resolving model was performed at the German high performance computing centers ZIB Berlin and LRZ Munich, supported by the German CLIVAR program.

References

Barnier, B., L. Siefridt, and P. Marchesiello, 1995: Thermal forcing for a global ocean circulation model using a three year climatology of ECMWF analysis. *J. Mar. Sys.*, **6**, 363–380.

Böning, C. W., F. O. Bryan, W. R. Holland, and R. Doescher, 1996: Deep-water formation and meridional overturning in a high-resolution model of the North Atlantic. *J. Phys. Oceanogr.*, **26**, 1142–1164.

Böning, C. W., W. R. Holland, F. O. Bryan, G. Danabasoglu, and J. C. McWilliams, 1995: An overlooked problem in model simulations of the thermohaline circulation and heat transport in the Atlantic ocean. *J. Climate*, **8**, 515–523.

Boyer, T. P. and S. Levitus, 1997: Objective analyses of temperature and salinity for the world ocean on a 1/4 degree grid. Technical report, NOAA Atlas NESDIS 11, U.S. Gov. Printing Office, Washington, D.C.

Chen, F. and M. Ghil, 1995: Interdecadal variability of the thermohaline circulation and high-latutude surface fluxes. *J. Phys. Oceanogr.*, **25**, 2547–2568.

Dengg, J., A. Beckmann, and R. Gerdes, 1996: *The Warmwatersphere of the North Atlantic Ocean*, chapter The Gulf Stream separation problem. Gebrueder Borntraeger, Berlin, Germany.

Dengg, J., C. W. Böning, U. Ernst, R. Redler, and A. Beckmann, 1999: Effects of an improved model representation of overflow water on the subpolar North Atlantic. *WOCE Newsletter*, **37**.

Eden, C. and C. Böning, 2002: Sources of eddy kinetic energy in the Labrador Sea. *J. Phys. Oceanogr.*. In press.

Eden, C. and R. J. Greatbatch, 2002: A damped decadal oscillation in the North Atlantic climate system. *J. Climate*. Submitted.

Ezer, T. and G. L. Mellor, 1994: Diagnostic and prognostic calculations of the North Atlantic circulation and sea level using a sigma coordinate ocean model. *J. Geophys. Res.*, **99**(C7), 14159–14171.

FLAME Group, 1998: FLAME- a Family of Linked Atlantic Model Experiments. Technical report, AWI Bremerhaven, Germany.

Ganachaud, A. and C. Wunsch, 2000: Improved estimates of global ocean circulation, heat transport and mixing from hydrographic data. *Nature*, **408**, 453–457.

Gargett, A. E., 1984: Vertical eddy diffusivity in the ocean interior. *J. Mar. Res.*, **42**, 359–393.

Gaspar, P., Y. Gregoris, and J.-M. Lefevre, 1990: A simple eddy kinetic energy model for simulations of the oceanic vertical mixing: tests at station PAPA and Long-Term Upper Ocean Study site. *J. Geophys. Res.*, **95**, 16179–16193.

Geshelin, Y., J. Sheng, and R. J. Greatbatch, 1999: Monthly mean climatologies of temperature and salinity in the western North Atlantic. *Can. Data Rep. Hydrogr. Ocean. Sci.*, **153**.

Greatbatch, R. J., A. F. Fanning, A. D. Goulding, and S.Levitus, 1991: A diagnosis of interpentadal circulation changes in the North Atlantic. *J. Geophys. Res.*, **96**, 22009–22023.

Griffies, S. M., 1998: The Gent-McWilliams skew flux. *J. Phys. Oceanogr.*, **28**, 831–841.

Griffies, S. M., R. C. Pacanowski, and B. R. Hallberg, 2000: Spurious diapycnal mixing associated with advection in a z-coordinate ocean model. *Mon. Wea. Rev.*, **128**, 538–564.

Kröger, J., 2001: *Mechanismen meridionaler Transportprozesse im tropischen Atlantik*. Ph.D. thesis, Universität Kiel, Institut für Meereskunde. Nr. 324.

Levitus, S. and T. P. Boyer, 1994: World Ocean Atlas 1994. Technical report, NOAA, U.S. Gov. Print. Off., Washington D.C,USA.

MacDonald, A. M. and C. Wunsch, 1996: An estimate of global ocean circulation and heat fluxes. *Nature*, **382**, 436–439.

Manabe, S. and R. J. Stouffer, 1988: Two stable equilibria of a coupled ocean–atmosphere model. *J. Climate*, **1**(9), 841–866.

Marotzke, J. and J. Willebrand, 1996: *The Warmwatersphere of the North Atlantic Ocean*, chapter The North Atlantic mean circulation: Combining data and dynamics. Gebrueder Borntraeger, Berlin, Germany.

Oschlies, A. and V. Garcon, 1999: An eddy–permitting coupled physical–biological model of the North Atlantic. 1. Sensitivity to advection numerics and mixed layer physics. *Glob. Biochem. Cycles*, **13**, 135–160.

Pacanowski, R. C., 1995: MOM 2 Documentation, User's Guide and Reference Manual. Technical report, GFDL Ocean Group, GFDL, Princeton, USA.

Paiva, A. M., J. T. Hargrove, E. P. Chassignet, and R. Bleck, 1999: Turbulent behavior of a fine mesh (1/12 degree) numerical simulation of the North Atlantic. *J. Mar. Sys.*, **21**, 307–320.

Sarmiento, J. L. and K. Bryan, 1982: An ocean transport model for the North Atlantic. *J. Geophys. Res.*, **87**, 394–408.

Sheng, J., R. J. Greatbatch, and D. Wright, 2001: Improving the utility of ocean circulation models through adjustment of the momentum balance. *J. Geophys. Res.*, **106**, 16711–16728.

Smith, R. D., M. E. Maltrud, F. O. Bryan, and M. W. Hecht, 2000: Numerical simulation of the North Atlantic Ocean at $1/10^o$. *J. Phys. Oceanogr.*, **30**, 1532–1561.

Stammer, D., P. R. Tokmakian, A. Semnter, and C. Wunsch, 1996: How well does a 1/4 deg global circulation model simulate large scale oceanic observations. *J. Geophys. Res.*, **101**, 25779–25811.

Stevens, D. P., 1990: On open boundary conditions for three dimensional primitiv equation ocean circulation models. *Geophys. Astrophys. Fluid Dyn.*, **51**, 103–133.

Stutzer, S. and W. Krauss, 1998: Mean circulation and transports in the South Atlantic Ocean: Combining model and drifter data. *J. Geophys. Res.*, **103**, 30985–31002.

Trenberth, K. and J. Caron, 2001: Estimates of meridional atmosphere and ocean heat transports. *J. Climate*, **14**, 3433–3443.

Veronis, G., 1975: The role of models in tracer studies. In: *Numerical Models of the Ocean Circulation*, pp. 133–146. National Academy of Sciences.

Willebrand, J., B. Barnier, C. Böning, C. Dieterich, P. Killworth, C. LeProvost, Y. Jia, J. M. Molines, and A. L. New, 2001: Circulation characteristics in three eddy-permitting models of the North Atlantic. *Prog. Oceanogr.*, **48**(2–3), 123–161.

Woodgate, R. A. and P. D. Killworth, 1997: The effects of assimilation on the physics of an ocean model. Part 1: Theoretical model and barotropic results. *J. Atm. Ocean. Techn.*, **14**(4), 897–909.

Figure captions

Fig. 1 Basin averaged kinetic energy density in cm^2/s^2 over the reference integration (13 years) of the eddy–permitting prognostic model.

Fig. 2 A one-dimensional example illustrating the principle effect of the original and the smoothed semi–prognostic method on possible data errors and mesoscale (model) features. Shown are isopycnals of the model density ρ_m (lower solid line), the climatological density ρ_c (upper solid line) and the dynamically active density ρ^* for the original semi–prognostic method (dashed line) and the smoothed semi–prognostic method (dotted line). Note that in contrast to the original

method, the smoothed method preserves the idealized mesoscale feature in ρ_m and suppresses the "data error" in ρ_c. Units for density (vertical axis) are arbitrary, the horizontal axis denotes a spatial dimension (in m).

Fig. 3 **a)**: Annual mean net surface heat flux in Wm^{-2} as given by the analysis of Barnier et al. (1995) driving the models as part of the surface (heat flux) boundary condition. Contour interval is 20 Wm^{-2} in–between and 50 Wm^{-2} beyond the interval $[-100, 100]$ Wm^{-2}. **b)**: 3–year mean diagnosed heat flux in the (prognostic) FLAME eddy permitting model. **c)**: same for the DYNAMO model. **d)**: same for the semi–prognostic (FLAME) model. All data has been spatially smoothed with a (2^o half–width) boxcar–window prior to plotting.

Fig. 4 **a)**: Annual mean climatological temperature taken from Boyer and Levitus (1997) at 50 m depth east of Newfoundland. Contour interval is 0.5 K in–between and 1 K beyond the interval $[6^o, 15^o]$ C. **b**: 3–year mean of temperature and velocities at the same depth in the prognostic model. **c**: same as b) but in the semi–prognostic model. **d**: same as b) but for a prognostic model with increased resolution ($1/12^o$ instead of $1/3^o$). Every second vector is shown for the $1/3^o$ models and every 8. th vector for the $1/12^o$ model.

Fig. 5 **a)**: Annual mean climatological temperature taken from Boyer and Levitus (1997) at 50 m depth. Contour interval is 1 K in the interval $[-2^o, 20^o]$ C and 2 K beyond. **b**: 3–year mean of temperature and velocities at the same depth in the prognostic model. **c**: same as b) but in the semi–prognostic model. **d**: same as b) but for a prognostic model with increased resolution ($1/12^o$ instead of $1/3^o$). Every second vector is shown for the $1/3^o$ models and every 8. th vector for the $1/12^o$ model.

Fig. 6 3–year averages of northward heat transport in PW in the eddy–permitting prognostic model (black, thick line) the DYNAMO model (red, thick line), the eddy–resolving model (green, thick line) and the semi–prognostic model (blue, thick line). Also shown are observational estimates of oceanic heat transports given by MacDonald and Wunsch (1996) (black circles with errorbars), by Ganachaud and Wunsch (2000) (red circles with errorbars) and by Trenberth and Caron (2001) (dashed, magenta line).

Fig. 7 3–year averages of the meridional streamfunction in $Sv = 10^6$ $m^3 s^{-1}$ for the eddy–permitting prognostic model (a) and the semi–prognostic model (b). Contour interval is 1 Sv. Note the stretched vertical axis above 800 m and 120 m.

Fig. 8 Eddy Kinetic Energy (EKE) at 50 m depth in m^2/s^2. Shown is the logarithm of EKE, i. e. values at contour lines are powers of 10; contour interval is 0.25. (a) shows EKE in the prognostic eddy–

permitting model, (b) to (d) EKE in semi-prognostic models using the original method (b), the mean (exp. MEAN) method (c) and the smoothed and tapered (exp. SMOOTH) method (d). EKE was calculated from velocity deviations from seasonal means and averaged over the 3–year analysis period. The data have been spatially smoothed with a (2^o half–width) boxcar–window prior to plotting.

Fig. 9 **a)** and **b)**: 3–year mean of temperature and velocities at 50 m depth in the mean semi–prognostic model (MEAN). Contour intervals, etc are the same as for Fig. 4 and Fig. 5 respectively. **c)**: 3–year mean diagnosed heat flux (similar to Fig. 3) for the mean and tapered semi–prognostic model (MEAN+SMOOTH-800).

Fig. 10 **a:** Mean northward heat transport in PW in the prognostic model (black), MEAN (red), SMOOTH (green), MEAN+SMOOTH (blue) and MEAN+SMOOTH-800 (magenta). **b:** Meridional streamfunction in MEAN+SMOOTH-800 in Sv. Contour interval is 1 Sv.

Fig. 11 **a:** Mean northward heat transport in PW in MEAN (red, solid), MEAN-CORR (red, dashed), MEAN+SMOOTH (blue, solid), MEAN+SMOOTH-CORR (blue, dashed), MEAN+SMOOTH-800 (magenta, solid) and MEAN+SMOOTH-800-CORR (magenta, dashed). **b:** Meridional streamfunction in MEAN+SMOOTH-800-CORR in Sv. Contour interval is 1 Sv.

Fig. 12 **a)** and **b)**: 3–year mean of temperature and velocities at 50 m depth in the corrected–prognostic model MEAN+SMOOTH-800-CORR. Contour intervals, etc are the same as for Fig. 5 and Fig. 4 respectively. **c)**: 3–year mean diagnosed heat flux (similar to Fig. 3) for the corrected–prognostic model (MEAN+SMOOTH-800-CORR).

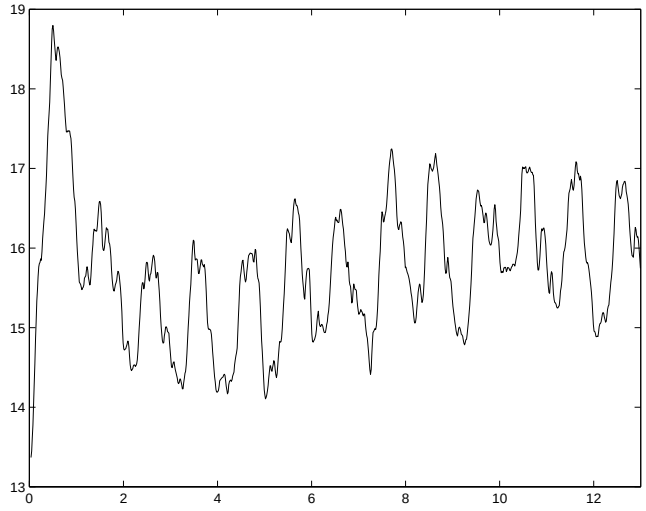

Figure 1: Basin averaged kinetic energy density in cm^2/s^2 over the reference integration (13 years) of the eddy–permitting prognostic model.

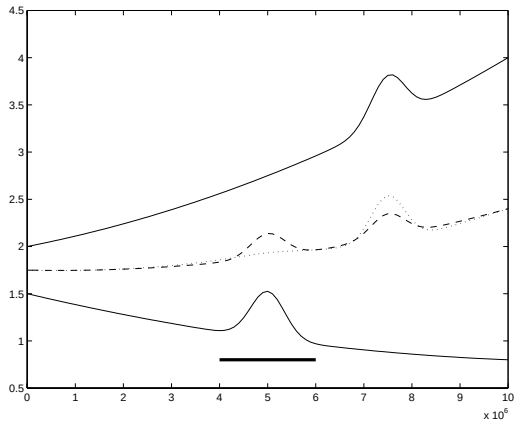

Figure 2: A one-dimensional example illustrating the principle effect of the original and the smoothed semi–prognostic method on possible data errors and mesoscale (model) features. Shown are isopycnals of the model density ρ_m (lower solid line), the climatological density ρ_c (upper solid line) and the dynamically active density ρ^* for the original semi–prognostic method (dashed line) and the smoothed semi–prognostic method (dotted line). Note that in contrast to the original method, the smoothed method preserves the idealized mesoscale feature in ρ_m and suppresses the "data error" in ρ_c. Units for density (vertical axis) are arbitrary, the horizontal axis denotes a spatial dimension (in m).

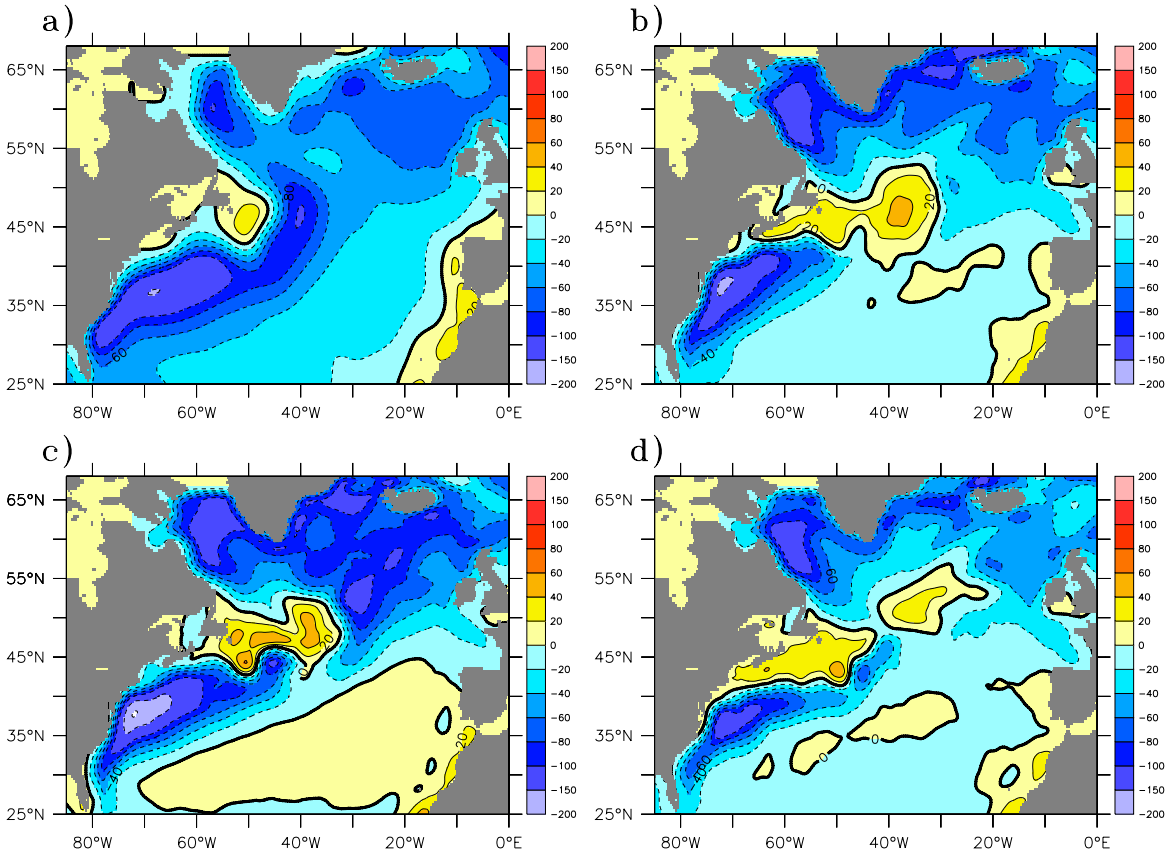

Figure 3: **a)**: Annual mean net surface heat flux in Wm^{-2} as given by the analysis of Barnier et al. (1995) driving the models as part of the surface (heat flux) boundary condition. Contour interval is 20 Wm^{-2} in–between and 50 Wm^{-2} beyond the interval $[-100, 100]$ Wm^{-2}. **b)**: 3–year mean diagnosed heat flux in the (prognostic) FLAME eddy permitting model. **c)**: same for the DYNAMO model. **d)**: same for the semi–prognostic (FLAME) model. All data has been spatially smoothed with a (2^o half–width) boxcar–window prior to plotting.

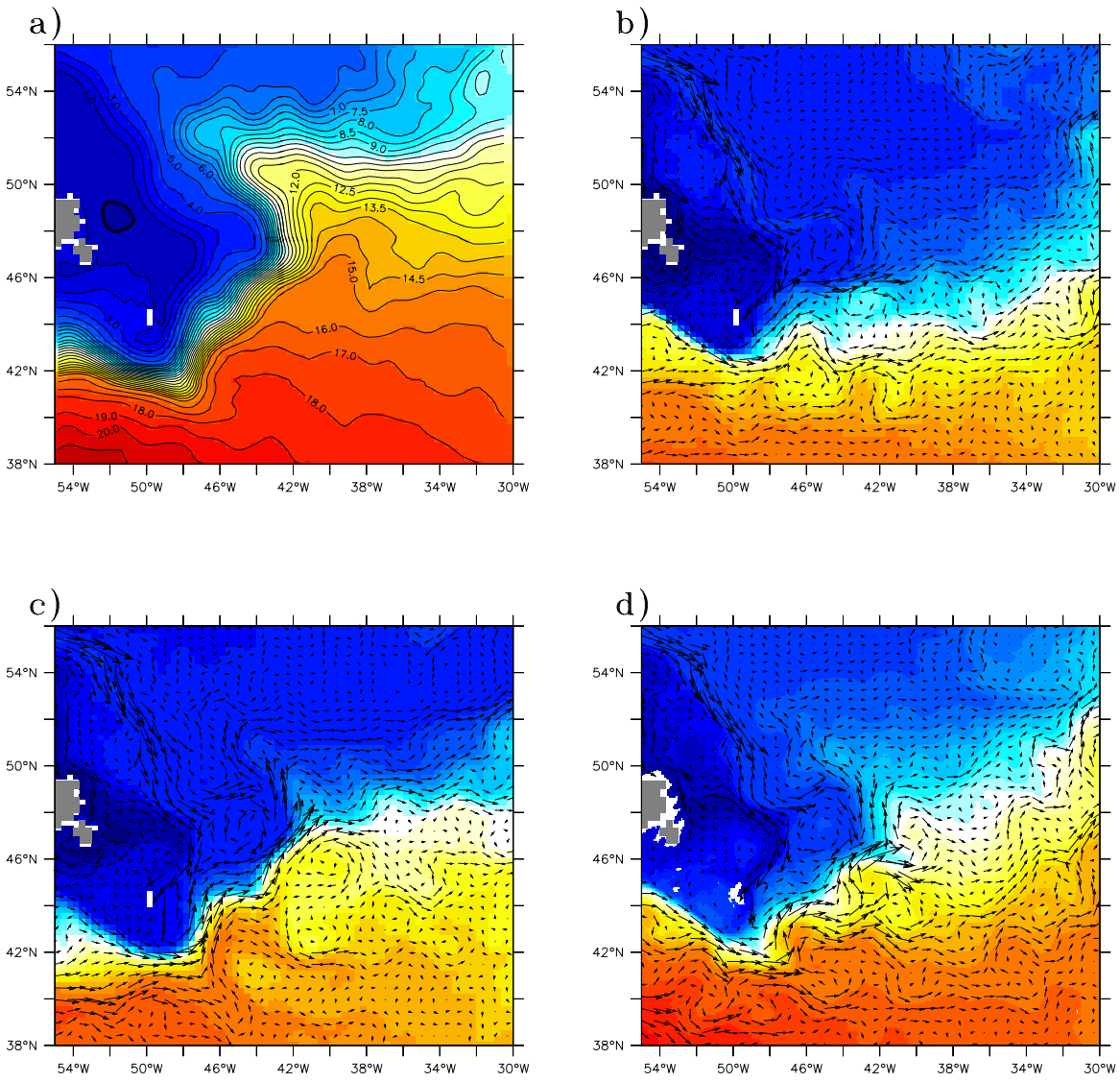

Figure 4: **a)**: Annual mean climatological temperature taken from Boyer and Levitus (1997) at 50 m depth east of Newfoundland. Contour interval is 0.5 K in–between and 1 K beyond the interval $[6^o, 15^o]$ C. **b**: 3–year mean of temperature and velocities at the same depth in the prognostic model. **c**: same as b) but in the semi–prognostic model. **d**: same as b) but for a prognostic model with increased resolution ($1/12^o$ instead of $1/3^o$). Every second vector is shown for the $1/3^o$ models and every 8. th vector for the $1/12^o$ model.

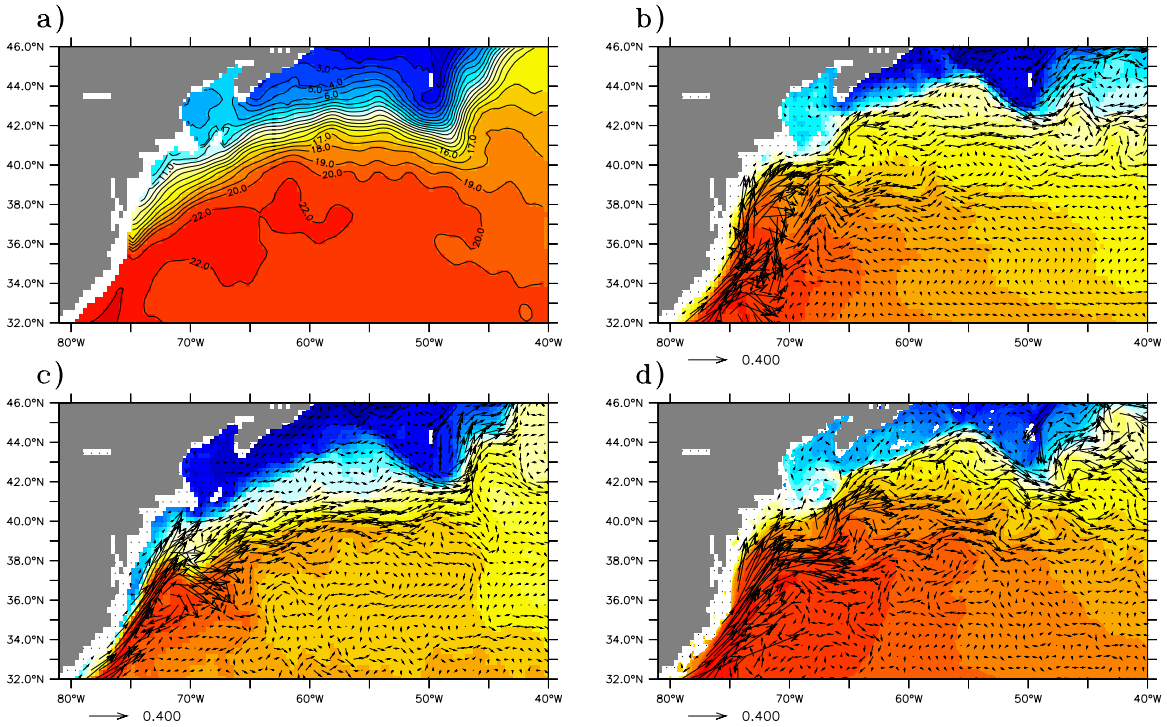

Figure 5: **a)**: Annual mean climatological temperature taken from Boyer and Levitus (1997) at 50 m depth. Contour interval is 1 K in the interval $[-2^o, 20^o]$ C and 2 K beyond. **b**: 3–year mean of temperature and velocities at the same depth in the prognostic model. **c**: same as b) but in the semi–prognostic model. **d**: same as b) but for a prognostic model with increased resolution ($1/12^o$ instead of $1/3^o$). Every second vector is shown for the $1/3^o$ models and every 8. th vector for the $1/12^o$ model.

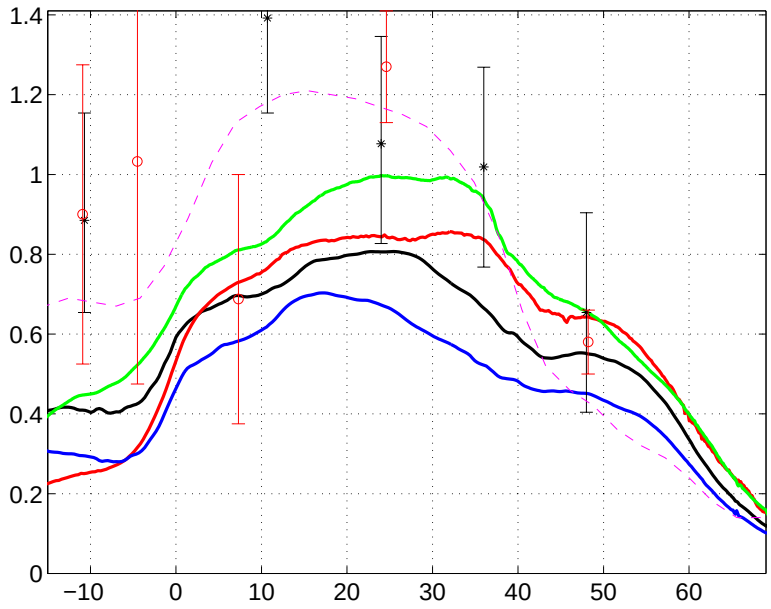

Figure 6: 3–year averages of northward heat transport in PW in the eddy–permitting prognostic model (black, thick line) the DYNAMO model (red, thick line), the eddy–resolving model (green, thick line) and the semi–prognostic model (blue, thick line). Also shown are observational estimates of oceanic heat transports given by MacDonald and Wunsch (1996) (black circles with errorbars), by Ganachaud and Wunsch (2000) (red circles with errorbars) and by Trenberth and Caron (2001) (dashed, magenta line).

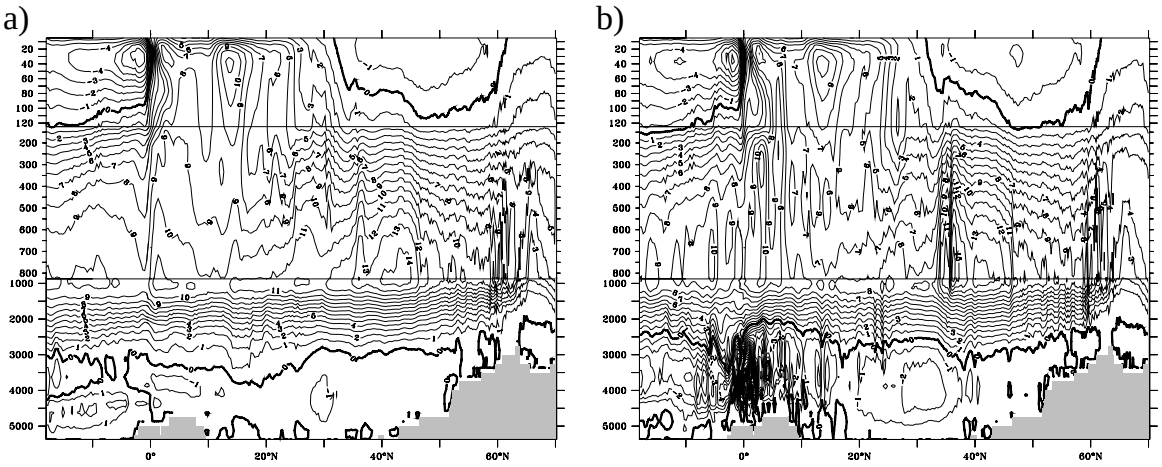

Figure 7: 3–year averages of the meridional streamfunction in $Sv = 10^6\ m^3 s^{-1}$ for the eddy–permitting prognostic model (a) and the semi–prognostic model (b). Contour interval is 1 Sv. Note the stretched vertical axis above 800 m and 120 m.

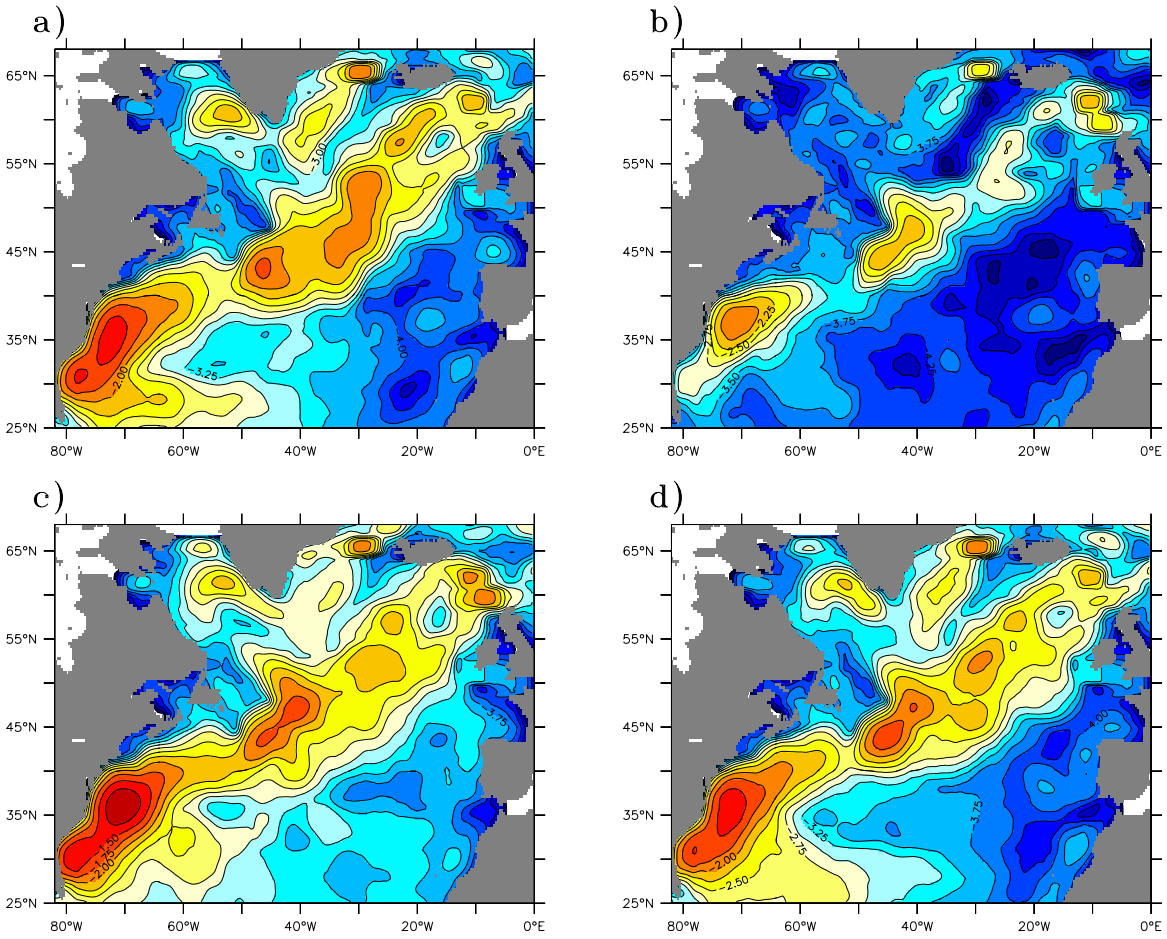

Figure 8: Eddy Kinetic Energy (EKE) at 50 m depth in m^2/s^2. Shown is the logarithm of EKE, i. e. values at contour lines are powers of 10; contour interval is 0.25. (a) shows EKE in the prognostic eddy–permitting model, (b) to (d) EKE in semi-prognostic models using the original method (b), the mean (exp. MEAN) method (c) and the smoothed and tapered (exp. SMOOTH) method (d). EKE was calculated from velocity deviations from seasonal means and averaged over the 3–year analysis period. The data have been spatially smoothed with a (2^o half–width) boxcar–window prior to plotting.

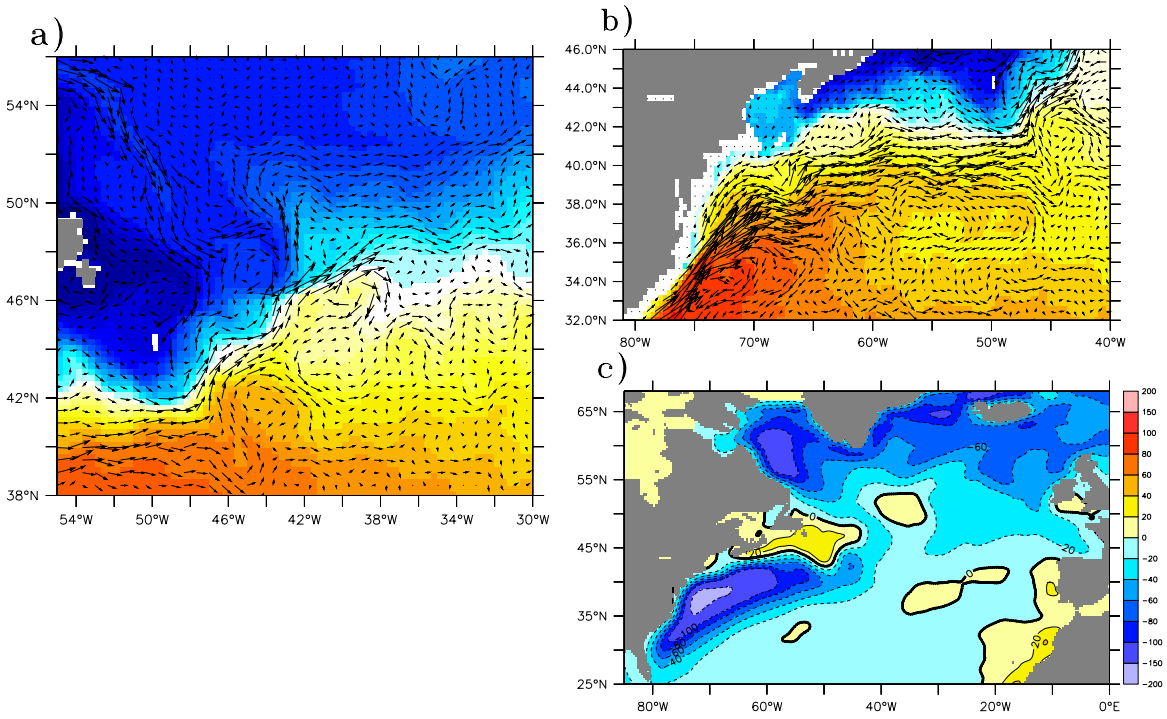

Figure 9: **a)** and **b)**: 3–year mean of temperature and velocities at 50 m depth in the mean semi–prognostic model (MEAN). Contour intervals, etc are the same as for Fig. 4 and Fig. 5 respectively. **c)**: 3–year mean diagnosed heat flux (similar to Fig. 3) for the mean and tapered semi–prognostic model (MEAN+SMOOTH-800).

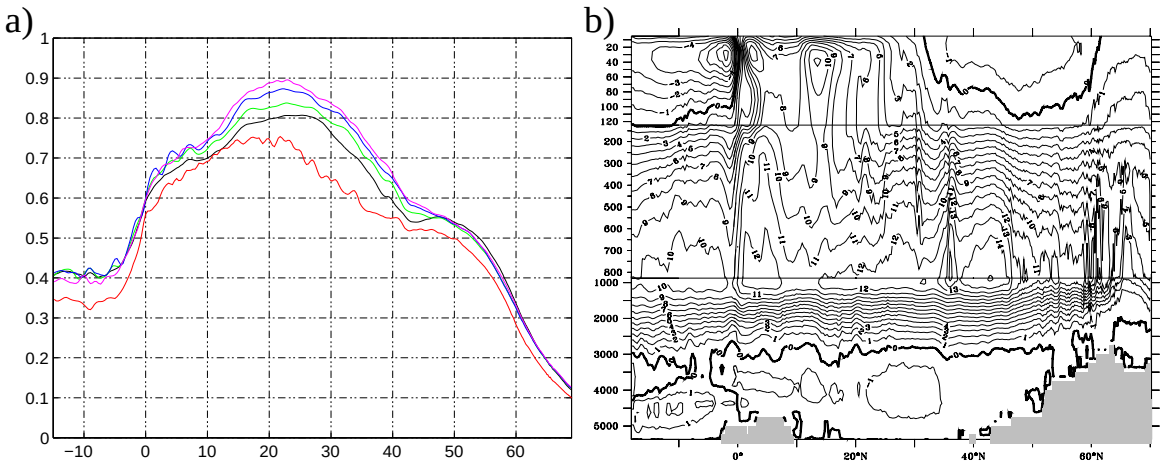

Figure 10: **a:** Mean northward heat transport in PW in the prognostic model (black), MEAN (red), SMOOTH (green), MEAN+SMOOTH (blue) and MEAN+SMOOTH-800 (magenta). **b:** Meridional streamfunction in MEAN+SMOOTH-800 in Sv. Contour interval is 1 Sv.

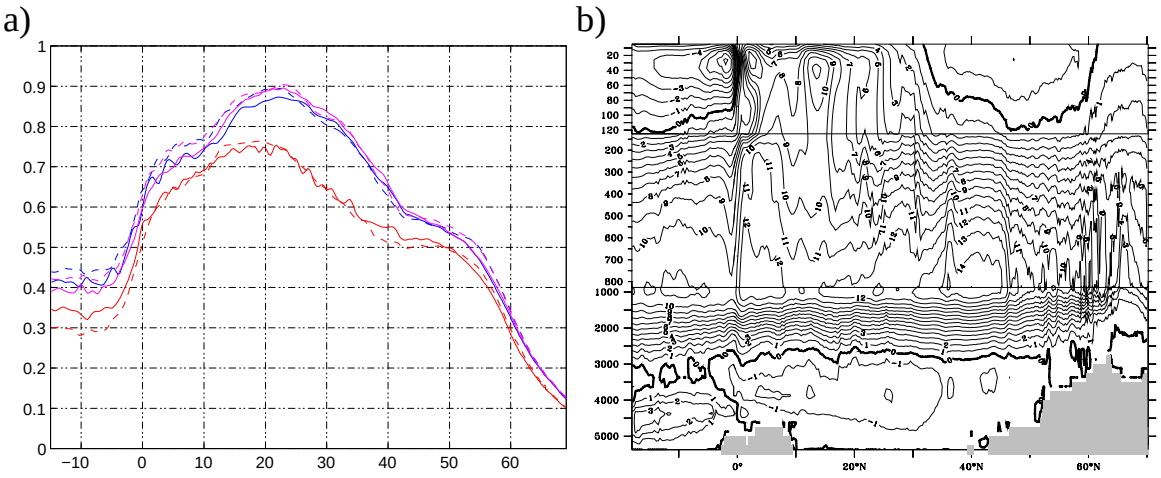

Figure 11: **a:** Mean northward heat transport in PW in MEAN (red, solid), MEAN-CORR (red, dashed), MEAN+SMOOTH (blue, solid), MEAN+SMOOTH-CORR (blue, dashed), MEAN+SMOOTH-800 (magenta, solid) and MEAN+SMOOTH-800-CORR (magenta, dashed). **b:** Meridional streamfunction in MEAN+SMOOTH-800-CORR in Sv. Contour interval is 1 Sv.

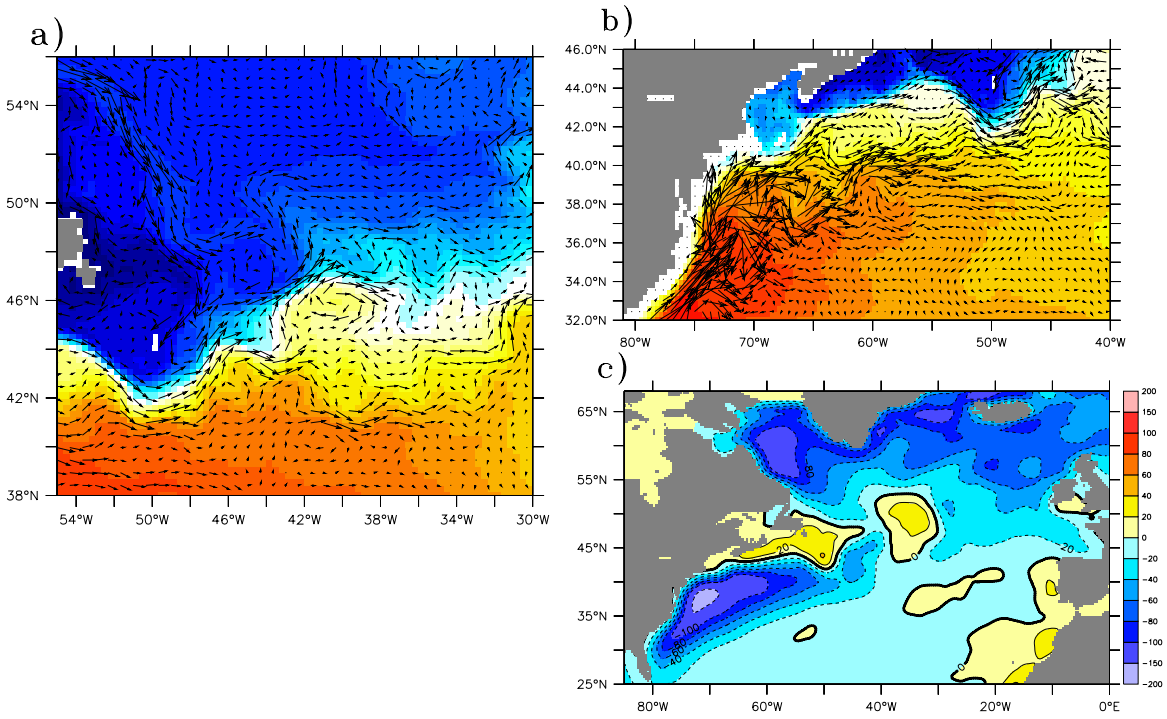

Figure 12: **a)** and **b)**: 3–year mean of temperature and velocities at 50 m depth in the corrected–prognostic model MEAN+SMOOTH-800-CORR. Contour intervals, etc are the same as for Fig. 5 and Fig. 4 respectively. **c)**: 3–year mean diagnosed heat flux (similar to Fig. 3) for the corrected–prognostic model (MEAN+SMOOTH-800-CORR).